Meteorol. Atmos. Phys. 56, 17–32 (1995)

Meteorology and Atmospheric Physics



Department of Meteorology, School of Ocean and Earth Science and Technology, University of Hawaii, U.S.A.

# Transition From a Cold to a Warm State of the El Niño-Southern Oscillation Cycle

**B. Wang**

With 9 Figures

Received October 20, 1993
Revised January 24, 1994

**Summary**

The transition from a cold to a warm state of the El Niño-Southern Oscillation (ENSO) cycle is studied using Comprehensive Ocean-Atmosphere Data Sets (COADS) for the period 1950–1992.

The onset of El Niño (November to December of the year preceding the El Niño) is characterized by an occurrence of minimum sea-level pressure anomalies in the subtropics around the "node" line of the Southern Oscillation. This pressure fall favors the formation of the anomalous cyclonic circulations over the western Pacific and leads to the establishment of anomalous westerlies in the western equatorial Pacific during the boreal spring of the El Niño year. The westerly anomalies then intensify and propagate into the central Pacific by the end of the El Niño year. This is an essential feature of the development of a basin-wide warming.

It is argued that the development of the equatorial westerly anomalies over the western Pacific may result from the thermodynamic coupling between the atmosphere and ocean. In boreal winter and spring the mean zonal winds change from westerly to easterly over the western equatorial Pacific. A moderate equatorial westerly anomaly initially imposed on such a mean state may create eastward SST gradients via changing rates of evaporational cooling and turbulent mixing. The equatorial SST gradients would, in turn, induce differential heating and zonal pressure gradients which reinforce the westerly anomalies. The feedback between the eastward SST gradients and westerly anomalies promotes the eastward propagation of the westerly anomalies.

## 1. Introduction

The anomalous warming of the eastern-central equatorial Pacific Ocean and along the South American coast (termed as El Niño in this paper) occurs concurrent with the weakening of the southeast trades, which is in turn tied to the simultaneous pressure fall in the southeast Pacific and pressure rise over Indonesia (a low-index phase of the Southern Oscillation (SO)). This interannual variation of the coupled atmosphere/ocean system is now popularly referred to as El Niño-Southern Oscillation (ENSO).

A central question concerning the nature and prediction of ENSO is how the turnabout from a cold to a warm state (or vice versa) takes place. After Bjerknes' (1966, 1969) pioneering studies, a considerable number of investigations were carried out to search for the "initial" changes or precursors in the atmosphere or/and ocean that may be responsible for an El Niño. A complete review of this topic is not attended but works that are most relevant to the present study are briefly discussed here.

After examining the El Niños of 1957–1958, 1965, and 1972, Wyrtki (1975) found that the South American coastal warming is not due to a local weakening of the southeast trades off Peru. He noticed that during the two years preceding the coastal warming excessively strong southeast trades build up warm water in the western Pacific. He hypothesized that in the southern winter of the year preceding the El Niño (year −1 hereafter), the wide-spread decrease of the southeast trades causes

a strong El Niño. This, however, does not explain the origin of an ENSO event because the weakening of the trades is a part of the atmospheric response to the anomalously high SST (Philander and Rasmusson, 1985). Barnett (1981) tested Bjerknes' and Wyrtki's ideas by studying statistical relations between ocean/atmospheric fluctuations. They concluded that measures of both Hadley and Walker cells can be hindcasted at a lead time of a few months but with low skill; some key features of trade winds are effective in hindcasting ocean variables at both short (0–3 months) and long (10–12 months) lead time.

Rasmusson and Carpenter (1982) made a comprehensive description of a composite ENSO scenario based on six events during 1950–1976. They found that equatorial easterly anomalies occur west of the dateline during the *antecedent* period from July to October of the year $-1$, and equatorial westerly anomalies occur over the western Pacific in the *onset* phase (around the end of year $-1$). They were puzzled by the appearance of SST anomalies near the dateline concurrent with the westerly anomalies in the onset. These westerly anomalies occurring in the equatorial western Pacific were suggested as a trigger of the South American coastal warming which may induce eastward-propagating Kelvin waves (Wyrtki, 1975; Philander, 1981, 1985; Busalacchi and O'Brien, 1981).

What is responsible for the initial changes in the western Pacific wind field? A variety of speculations has been made, including the twin cyclones which developed in the western-central Pacific (Keen, 1982), the persistent development of intraseasonal oscillations (Lau and Chan, 1986), the impacts of the cold surges from the east Asian winter monsoon (Lau et al., 1983), and the enhancement of the Australian summer monsoon (Hackert and Hastenrath, 1986).

In a series of studies, Barnett (1983, 1984, 1985) suggested that the surface wind and sea-level pressure (SLP) anomalies, which eventually cause most of the change in SST in the equatorial Pacific, originate in the equatorial Indian Ocean and propagate slowly eastward into the Pacific. The eastward propagation of the zonal wind anomalies above the boundary layer from the southeast Asian monsoon region to the western Pacific described by Yasunari (1985, 1990) and Gutzler and Harrison (1987) seem to support this notion. An interpretation was offered by Meehl (1987) in which the important role of the biennial variation of the monsoon circulation is emphasized. Trenberth and Shea's (1987) analysis of long record SLP data, on the other hand, revealed that the most dominant feature of the Southern Oscillation (SO) is a standing seesaw, and the eastward propagation of SLP anomalies is not very regular and is not supported by the long-term record. They showed that changes over the South Pacific pole of the SO lead opposite changes in the Indonesian pole by one to two seasons, with the largest lead of three seasons beginning near New Zealand. Possible South Pacific roles in ENSO onset were discussed by van Loon and Shea (1985, 1987), Trenberth and Shea (1987) and Kiladis and van Loon (1988).

It appears that the exact origin of the equatorial westerly anomalies in the western Pacific and their roles in ENSO development have not yet been firmly determined and well understood. The purpose of the present study is to search for common characteristics and possible causes of the transition from a cold to a warm state of the ENSO cycle by examining all the major events during 1950–1992.

The ENSO cycle is highly nonstationary. Each El Niño has its own characteristics. It is more meaningful to investigate the evolution of ENSO event by event. Case studies are also desirable for revealing the differences from case to case, which are valuable for understanding the nature and cause of the deviations from a composite scenario. Section 2 will show that the available Comprehensive Ocean-Atmosphere Data Set (COADS) is adequate for a case analysis of the six most significant ENSO events in the last four decades. These warm events include 1957, 1965, 1972, 1982, 1986–1987, and 1991 El Niños. Section 3 displays phase propagation diagrams for the six most significant warm events in an attempt to trace the origins of the ENSO anomalies. A detailed documentation of the common characteristics is followed in Section 4. A hypothesis regarding the development of the warm (ENSO) episode is proposed for further theoretical and numerical investigations in Section 5. The last section summarizes the results and discusses questions remaining open for future studies.

## 2. Data

The data used in the present study include monthly mean SST, SLP, and surface winds from COADS for the period 1950–1992. The analysis domain covers the tropical Indian and Pacific Oceans between 30° S and 30° N and from 40° E to 80° W. Original data were on 2° latitude by 2° longitude grid. To make a more reliable estimation of monthly means, the 2° × 2° data were combined into 5° (lat.) × 15° (log.) data by making observation number-weighted box averages. For the purpose of describing the planetary-scale ENSO anomalies, this resolution is adequate. The averaged monthly observations in each box for the period January 1950-December 1992 are more than 20 with the exception of seven boxes located in the equatorial eastern-central Pacific (Fig. 1a). The data density increased dramatically from 1955 to 1958 as shown for the seven worst boxes (Fig. 1b). In general, the data are adequate for case analyses of the six most significant ENSO events (1957–1958, 1965, 1972, 1982–1983, 1986–1987, and 1991) because of a relatively large number of observations and a high signal-to-noise ratio. Weaker warm events such as 1963 and 1969 not only have smaller amplitude but also smaller spatial scales, and it appears to have been more difficult to detect reliable signals.

The first step of data-quality control was based on a temporal consistency principle. A spatial interpolation scheme, which combines Laplacian interpolation with Cubic Spline fitting, was first used to make up all missing data in each box, if any. Annual cycle and monthly mean anomalies (MMA) were then computed for each variable at each box. It was assumed that monthly mean values that were computed from more than 30 observations were "reliable". If the observation was less than 15 per month and the difference between the MMA and its three-month running mean exceeded two standard deviations of the MMA, or if the observation number was between 15 and 30 and the difference was higher than 1.5 standard deviation, the MMA under consideration was regarded as unreliable and removed. After the removal of all unreliable data, a temporal interpolation scheme was used to make up the deleted data.

Further quality control was done based on a spatial consistency principle. The MMA's that exceeded the average of the corresponding four adjacent boxes by more than two standard deviations were weeded out as unreliable if the corresponding monthly observation number was below 40. Such unreliable values were then replaced by spatially interpolated values. A nine-box weighted mean was used to smooth the anomaly field after the spatial interpolation. The weight is 0.72 for the central box, 0.06375 for the adjacent four boxes, and 0.0056 for the other four boxes.

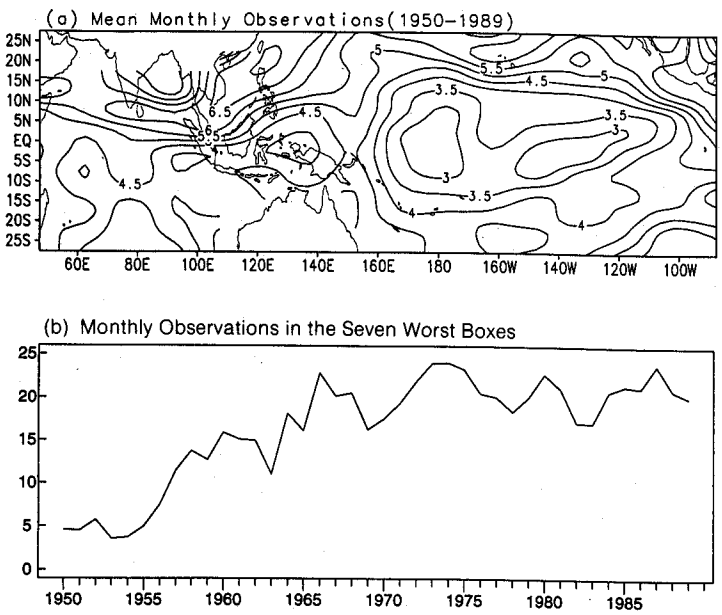


Fig. 1. (a) COADS monthly observations averaged for the period 1950–1989 and for each 5° latitude by 15° longitude box. Values of contours are shown in natural logarithm. The areas of less than three in the central Pacific indicate that the mean monthly observation is less than 20. (b) Mean monthly observation averaged for the seven most data-sparse boxes in the central Pacific as a function of time

To focus on ENSO variability, a low-pass Sharpiro (1970) filter was used to obtain a low-frequency component of the MMA series. Such a low-pass filtered time series is very similar to a 13-month running mean of the MMA series.

Based on a composite scenario derived from six warm events which occurred during 1950–1976, Rasmusson and Carpenter (1982) defined five phases for a warm event: Antecedent (June–October of year −1), onset (November of year −1 to January of year 0), peak (March–May of year 0), transition (June–October of year 0), and mature (November of year 0–February of year +1). They named March–May of year 0 as the peak phase because the South American coast reaches its peak warming during that period for the pre-1977 events. In view of the fact that there was no obvious coastal warming prior to the central Pacific peak warming (mature phase) in the latest three events, the boreal spring of year 0 will be called the *development* phase. All other terminologies (antecedent, onset, transition, and mature) will follow Rasmusson and Carpenter's (1982) definitions.

## 3. Phase Propagation of ENSO Anomalies

The spatial distribution of the extreme phases of SST, SLP, and surface zonal wind anomalies are examined in this section in an attempt to identify origins and propagation of ENSO anomalies. The phase diagram is a useful tool for tracing initial changes during the transition of the ENSO cycle. Caution, however, must be exercised when interpreting the phase propagation, because the anomalies are departures from climatological annual cycles. The annual cycles vary with time and space, and propagation of the anomalies might reflect annual variations.

### *3.1 The Peak Warming*

Figure 2 shows the phase of the locally highest anomalous SST (peak warming) for each of the six most significant El Niños. Significant peak warming that exceeds one-half of the standard deviation is confined to the east of the dateline along the equator. The phase discontinuity (thick lines on Fig. 2) indicates the spatial domain of the major ENSO warming.

There are salient differences in the phase propagation within the major warming areas between the pre-1977 and post-1977 episodes. The pre-1977 El Niños, which include 1957, 1965, and 1972 events, started from an amplification of the annual cycle along the South American coast. Peak warming occurs first off coast of Peru (20° S, 85° W) from March to May of the year 0, and off the coast of Ecuador (Equator and 85° W) four months later. The peak warming then takes place progressively later westward along the equator, and by the end of year 0 reaches the central Pacific. The anomalies propagate northward at a speed of about 4° latitude per month whereas westward at a speed of about 20° longitude per month. This propagation partially reflects the absence of the northwest propagation of the annual cooling in the Pacific cold tongue region. The 1976 warm event fits in with these features very well, except for a weaker central Pacific warming (figure not shown).

The post-1977 warming, including 1982, 1986–1987, and 1991 events, on the other hand, appears to be of equatorial origin. The peak warming either propagated eastward with a speed about 20° longitude per month in the 1982 event, or occurred nearly synchronously in the eastern-central equatorial Pacific in the events of 1986–1987 and 1991. In all three cases, the occurrence of the peak warming in the far eastern Pacific is in the boreal spring of the year +1.

There are also important differences outside the major warming regions between the pre- and post-1977 El Niños. In the pre-1977 events, a peak warming occurred in northern Australia and South Pacific Convergence Zone (SPCZ) during the boreal spring or summer of year −1 (Fig. 2). In the post-1977 events a noticeable peak warming occurred in the equatorial Pacific west of or near the dateline during the boreal fall or winter of year −1. Note also that from the onset to development phase (January to May of year 0), the post-1977 events exhibit peak warming in the northern and/or southern flank of the major warming regions. This feature is, however, absent for three pre-1977 events.

### *3.2 The Minimum Anomalous SLP*

The occurrence of the minimum SLP anomaly in the eastern-central Pacific south of the equator (0–15° S, 155°–110° W) is nearly in phase with the central Pacific warming (Fig. 3). The area

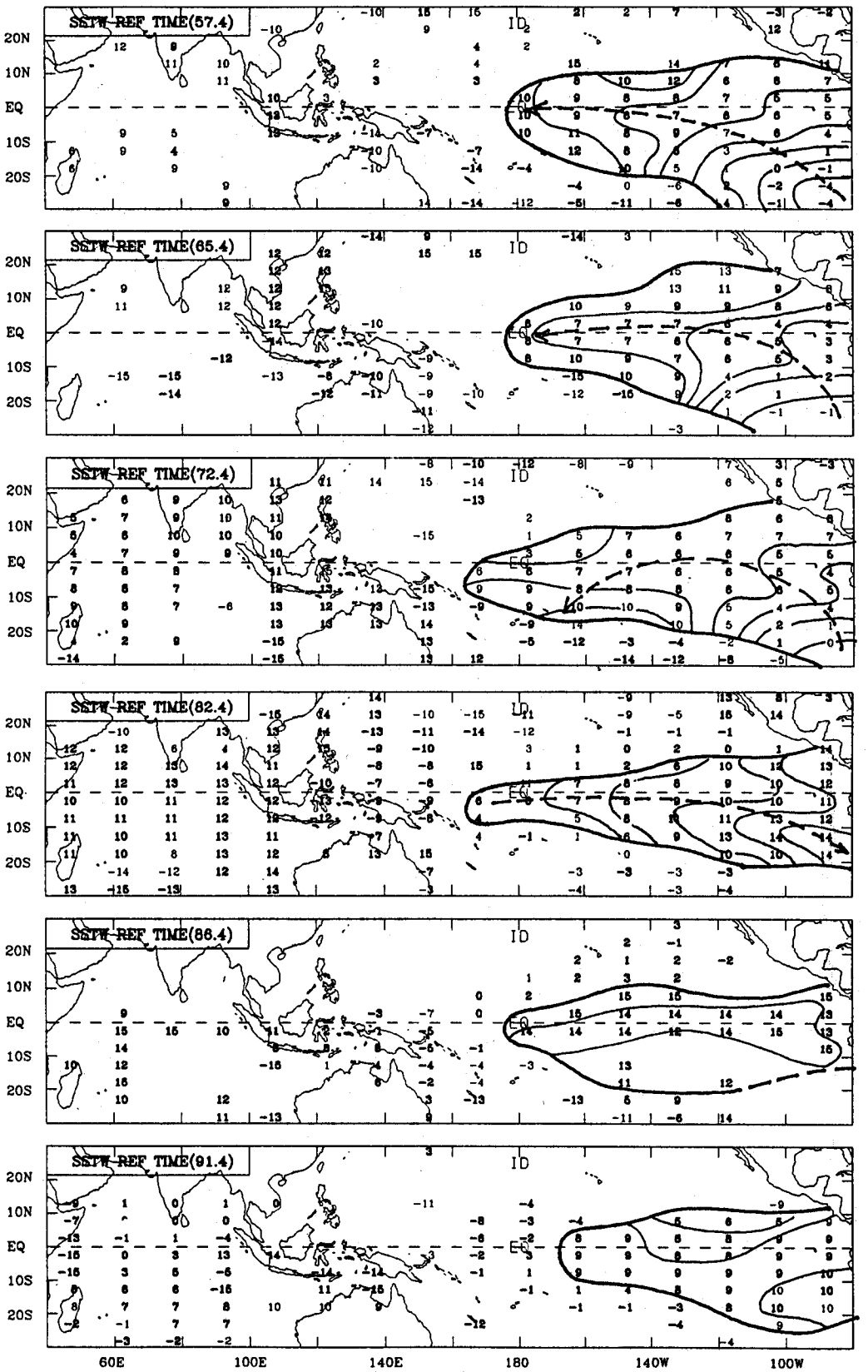


Fig. 2. Phase diagrams of SST anomalies showing the time of occurrence of the highest anomalous SST for the 1957, 1965, 1972, 1982, 1986–1987, and 1991 warm events. The time of occurrence is given by the number of the month that lags (positive) or leads (negative) the reference time given on the upper left corner of each panel. Heavy (light) letters denote that the extreme exceeds one (one-half) standard deviation. Blank areas imply no extreme or an extreme less than one-half standard deviation during the period from −15 to +15 months. Arrows indicate the direction of the phase propagation. Thin lines are constant phase lines. Thick lines are phase discontinuous lines separating different regimes

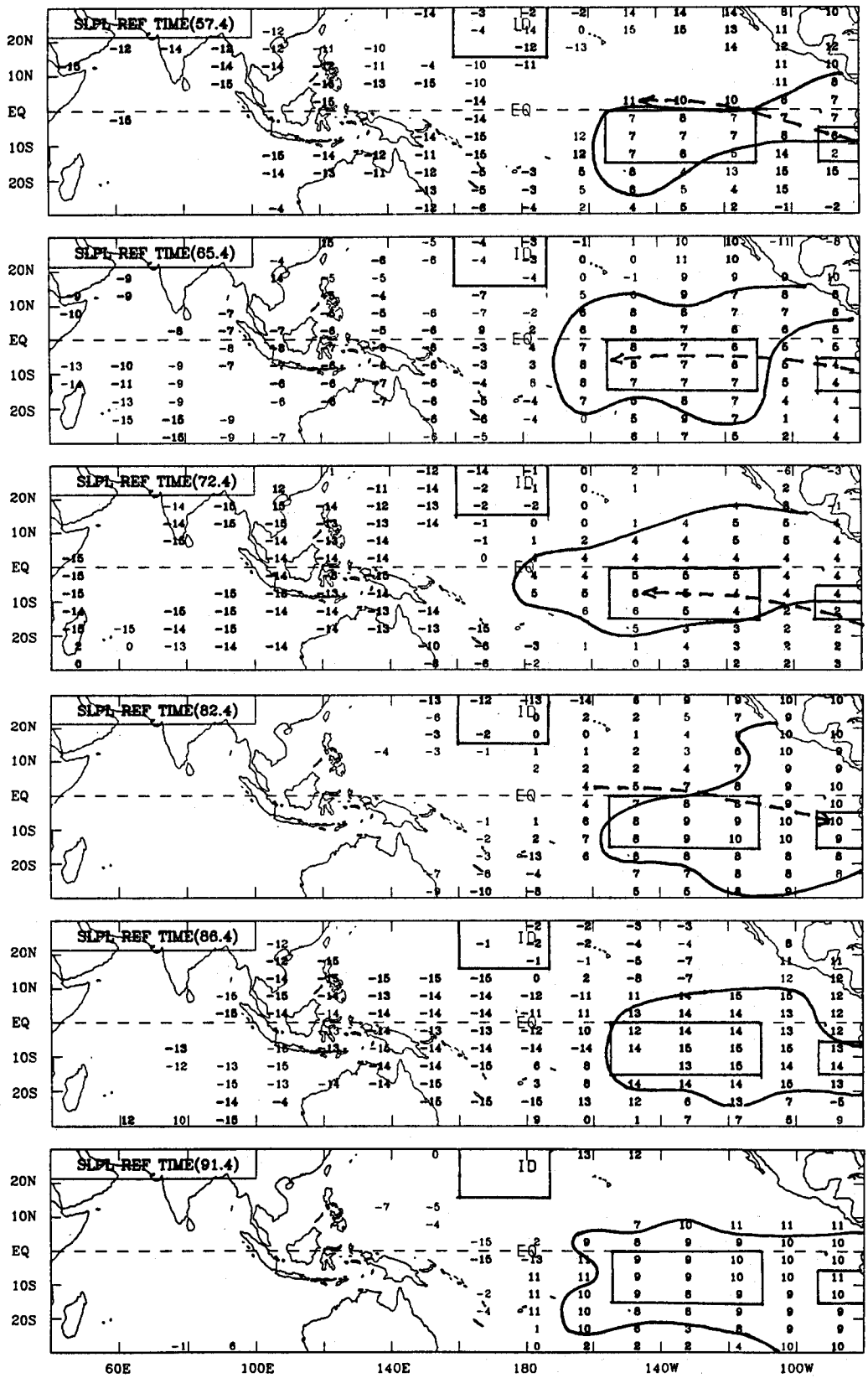


Fig. 3. As in Fig. 2 except for the lowest anomalous sea-level pressure. The areas enclosed by the thick solid curves indicate the regions where the minimum SLP anomalies occur nearly simultaneously

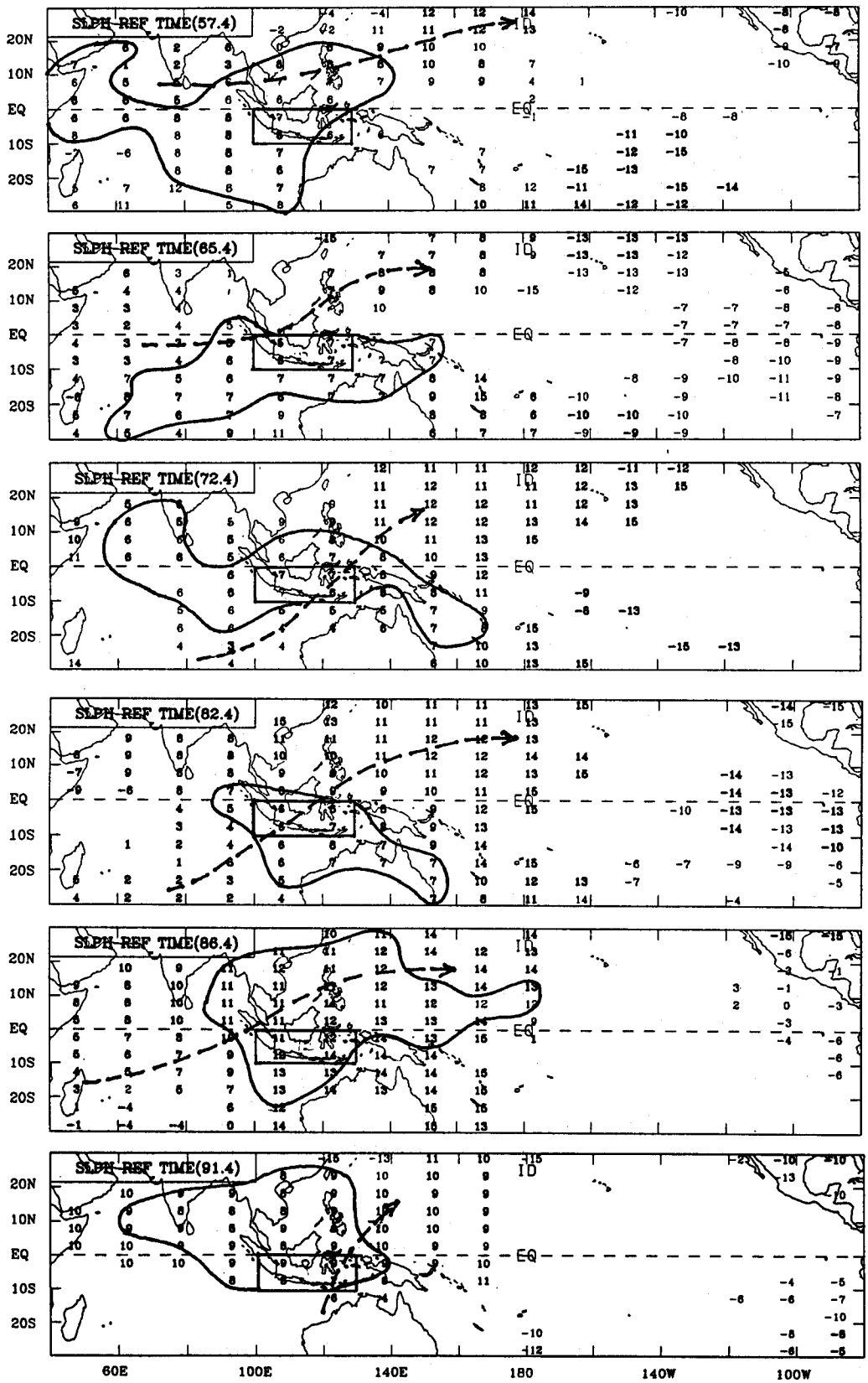


Fig. 4. As in Fig. 3 except for the highest anomalous sea-level pressure

where peak low occurs tends to coincide with the region of highest SST anomalies with a bias toward the southeast Pacific pole of the SO. In addition, although the minimum pressure tends to occur simultaneously, there are signs of westward propagation in the pre-1977 events, whereas there are signs of either eastward propagation (1982 and 1991) or remaining nearly stationary (1986–1987) in the post-1977 events. This indicates the coherency between SLP and SST anomalies.

Note that the minimum SLP anomalies in the central North Pacific (15–30° N, 160° E–170° W) occur in the boreal winter of year −1. This pressure fall leads the central Pacific warming by about one year for all events except the 1991 event (Fig. 3). This is probably the most notable precursor for El Niños. Also notable are the minimum SLP anomalies that occurred in the southern subtropics near the dateline (15–30° S, 160° E–170° W) for all pre-1977 events.

### *3.3 The Maximum Anomalous SLP*

The occurrence of maximum SLP anomalies over Indonesia (0–10° S, 100–130° E) tends to lead the central Pacific peak warming by one or two months (Fig. 4). Although the pressure peak occurs nearly synchronously in a large area, the size and the geographic location of the area vary significantly from event to event. There is an unmistakable northeastward phase propagation of the pressure peak from south of Sri Lanka (in the first two events) or southern Indian Ocean (in the last four events) across the Maritime Continent to the northwestern Pacific. The pressure obtains a maximum in the northwestern Pacific (10–25° N, 130–175° E) about three to seven months after the central Pacific peak warming. Barnett (1983, 1984, 1985) has documented an eastward propagation of the anomalous pressure using complex empirical orthogonal function (EOF) analysis. Note that the propagation described by the phase diagram here exhibits a significant northward component, in particular for the events after 1970. This propagation differs from the annual march of monsoonal low pressures which is in a northwest-southeast direction (Meehl, 1987).

What causes the northeastward propagation of the anomalous high? This question may be answered by addressing the following two questions: What causes the pressure rise in the Indian Ocean leading that in Indonesia? Why does the pressure rise in the northwestern Pacific follow that over Indonesia? The answer to the first question is unknown and probably not a simple one. In particular, why was the propagation path changed after 1970? The second question is easier to answer based on Bjerknes' (1969) conceptual framework. The occurrence of the anomalous SLP peak over the Indonesia is almost concurrent with the central Pacific peak warming in the boreal winter of year 0. Due to the eastward shift of the updraft of the Walker cell, the northern winter Hadley cell is enhanced. As a result the northern subtropical high should be strengthened after the peak warming. In other words, the occurrence of the anomalous SLP peak in the northwestern Pacific should lag that over Indonesia.

### *3.4 The Maximum Westerly Anomalies*

The westerly anomalies in the central Pacific (5° S–5° N, 170–155° W) are almost in phase with the peak warming in situ (Fig. 5). About four to nine months prior to the central Pacific peak warming, a pronounced maximum westerly anomaly occurs in the western Pacific just north of New Guinea (0–5° N, 130–145° E). The propagation is best identified in the equatorial western-central Pacific from 130° E to 170° W. Note that in most cases, there is a phase discontinuity (phases of two adjacent boxes differ by more than five months) around 130° E between Borneo and New Guinea (as marked out on Fig. 5) except in the event of 1965. West of the phase discontinuity from the central equatorial Indian Ocean to Borneo (5° S–5° N, 70–115° E), the maximum westerly anomalies occur in April to October of year −1, about six to twelve months earlier than the westerly anomalies peak that appears north of the New Guinea (0–5° N, 130–145° E).

A major difference that distinguishes the pre-1977 from post-1977 events is the prominent maximum westerly anomalies occurring in the southeast Pacific (0–20° S, 125–95° W) around the December of year −1. This maximum relaxation of southeast trades leads the warming off the South American coast by about one season. It may be an important cause for the coastal warming in the pre-1977 events, because in all the post-1977 events there is no such weakening of the southeast trades in the onset phase and, consequently,

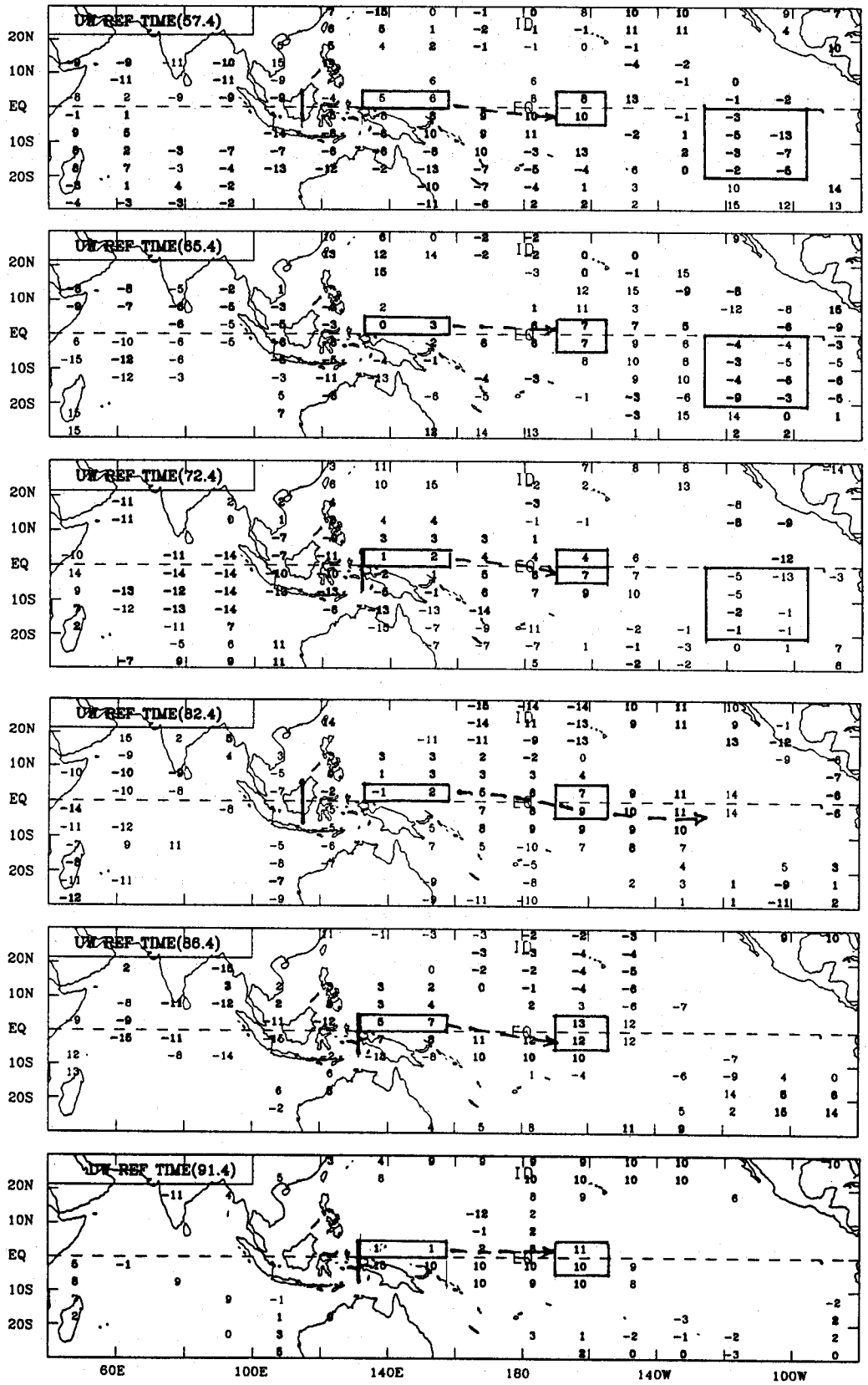


Fig. 5. As in Fig. 2 except for the maximum westerly anomalies

no coastal warming precedes the central Pacific warming.

## 4. Common Features of the ENSO Onset and Development

Regardless of the differences between the pre- and post-1977 warm events, common characteristics in the transition from a cold to a warm state of the ENSO cycle can be found, which are summarized in Fig. 6 and discussed in this section.

As noticed by Wyrtki (1975), about 15–30 months prior to the central Pacific warming, easterly anomalies attain their maximum over the equatorial Pacific (5° S–5° N, 160° E–95° W), and so do the westerly anomalies over the Maritime Continent and eastern Indian Ocean (5° S–5° N, 70–115° E) (Fig. 5). The location, strength, and timing of the peak equatorial easterly anomalies, however, vary tremendously from case to case (figure not shown). This leads to a moderate lag correlation coefficient of 0.41 between the anomalous equatorial easterly and the anomalous SST in the central Pacific with the easterly leading the warming by about 22 months (Fig. 7a). This coefficient is statistically significant at the 0.99 confidence level. The excessively strong trades during year −1 or −2, however, occur in concert with a La Nina or La Nina-like condition in the Pacific. There is no evidence that the collapse of equatorial easterlies in the central Pacific leads the Pacific warming, because the simultaneous correlation coefficient between the equatorial zonal wind anomalies and the SST anomaly at the central Pacific is 0.91. Therefore, those anomalies cannot be used as a predictor for the occurrence of a warm event.

The most conspicuous common signal that precedes the Pacific warming for all six strong warm events, is the decrease of SLP in the subtropics of each hemisphere near the "node" line of the SO (around the dateline). The anomalous SLP there, particularly in the north Pacific (15–30° N, 160° E–170° W), tends to reach a minimum about one year ahead of the central Pacific peak warming (Fig. 4). The maximum correlation coefficient is −0.54 with negative pressure anomalies at (15–30° N and 15–30° S, 160° E–170° W) leading the central Pacific warming by about 14 months (Fig. 7b). The weakening of the subtropical ridge near the dateline occurs during the northern winter of year −1 when the central equatorial Pacific SST is close to normal. It is, therefore, unlikely that the equatorial oceanic thermal forcing causes the attenuation of the subtropical ridge. Anomalous midlatitude winter circulation may directly alter the strength of the northern subtropical ridge, providing a mechanism that triggers ENSO onset and induces irregularities in the period of the SO.

Another prominent common feature is the occurrence of the maximum westerly anomalies north of New Guinea around the boreal spring of year 0. The lag correlation coefficient is 0.56 (sample size 504) between the equatorial westerly anomalies north of New Guinea and the central Pacific SST anomaly, with the westerly leading the warming by 7–8 months (Fig. 7c). Thereafter, the maximum westerly anomalies occur progres-

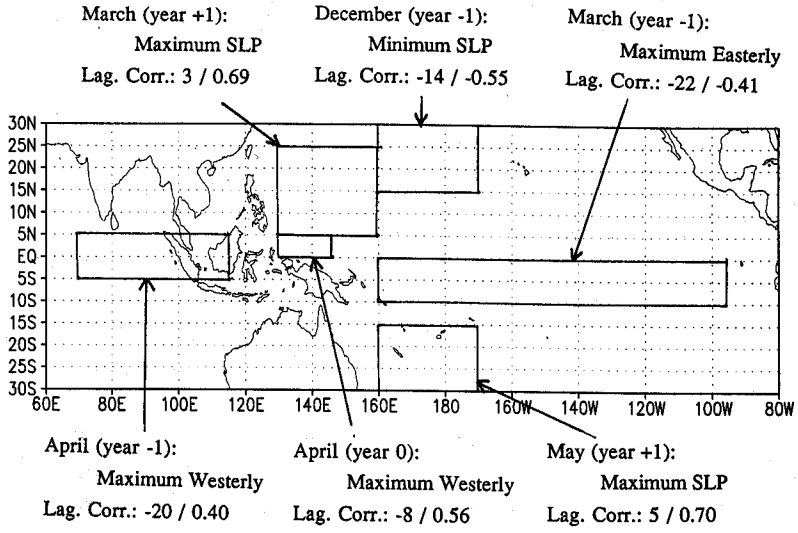


Fig. 6. A schematic diagram showing the areas where surface wind or SLP have best lag correlations with the central Pacific SST anomaly. The integer in the numerator denotes the phase leading of the variable with regard to the central Pacific SST anomaly in units of month, and the fraction in the denominator represents the lag-correlation coefficient

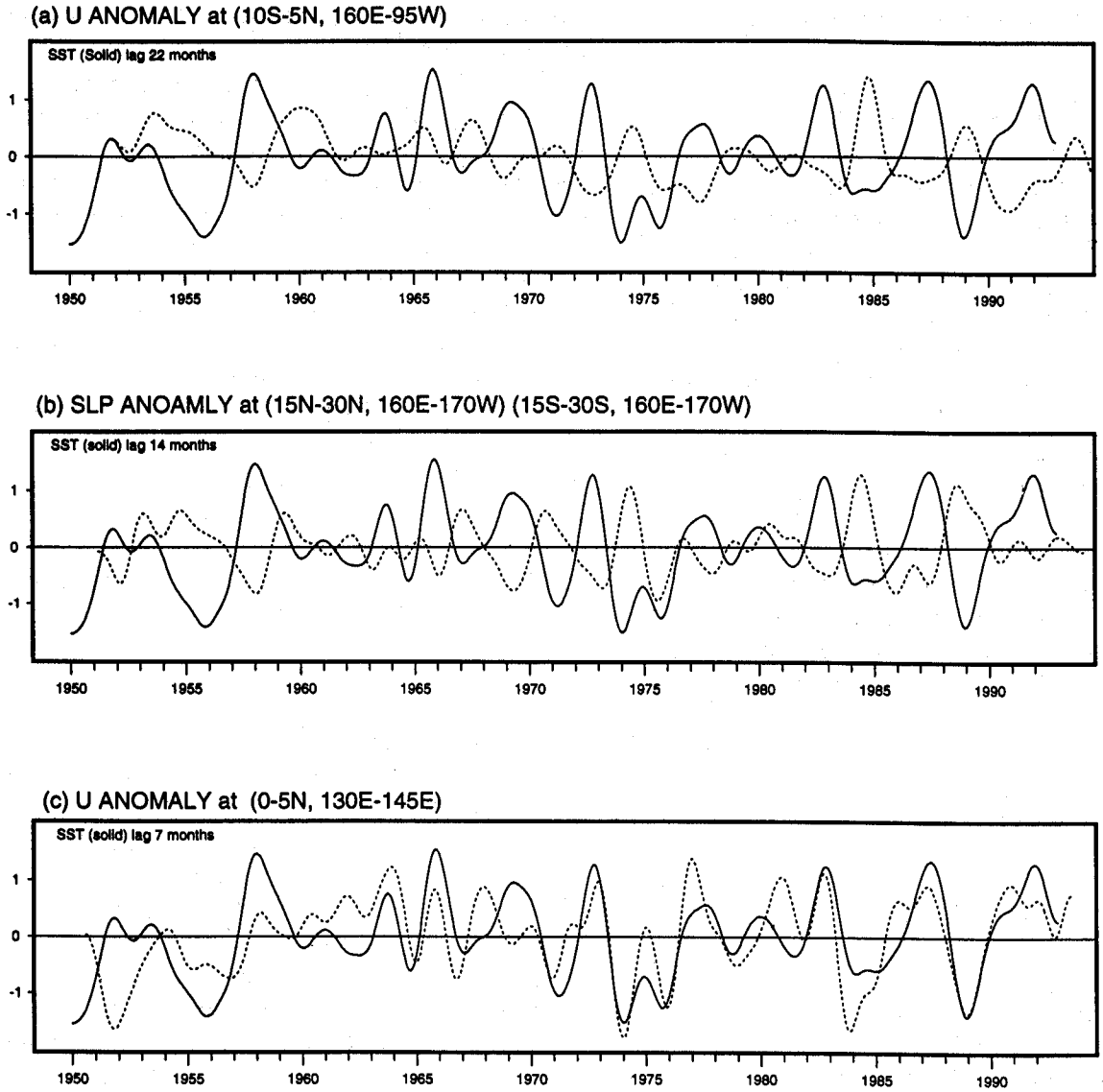


Fig. 7. The SST anomaly in the central Pacific (5° S–5° N, 170–155° W) (solid curves in all panels) and (a) the westerly anomaly in the equatorial Pacific (10° S–5° N, 160° E–95° W) (dashed); (b) the SLP anomalies in the subtropics near the node line of the Southern Oscillation (15–30° S and 15–30° N, 160° E–170° W) (dashed); and (c) the westerly anomalies north of New Guinea (0–5° N, 130–145° E) (dashed). Note that the dashed lines have been shifted forward in time by 22 months in (a), 14 months in (b), and 7 months in (c). All data are low-pass filtered (similar to a 13-month running mean)

sively later eastward along the equator as has been shown by the phase diagram (Fig. 5). By the mature phase, the maximum westerly anomalies are nearly in phase with the maximum SST anomaly in the central Pacific.

It is also noteworthy that pressure anomalies at the northwestern (10–25° N, 130–175° E) and south-western Pacific (15–30° S, 160° E–170° W) reach a peak about two to six months after the central equatorial Pacific peak warming (Fig. 3). The lag correlation coefficient is about 0.70 with northwestern (southwestern) Pacific positive pressure anomalies lagging the central Pacific warming by three (five) months. This results from the enhanced Hadley circulation that is associated with the anomalous heat source as suggested by Bjerknes (1966). The reinforcement of the high pressures in the western Pacific of each hemisphere leads to a recovery of the equatorial easterlies in the western Pacific and a decay of the warming.

## 5. A Hypothesis on ENSO Development

A common feature of ENSO development is the intensification and eastward propagation of the equatorial westerly anomalies in the western Pacific. This is true for all warm episodes during 1957–1992 (Fig. 8). Several features are noticeable. First, the initial westerly anomalies that occurred during the onset or early development phases are primarily confined to the west of the dateline and are not of basin-wide scale. Second, for the majority of the El Niños, the strongest westerly anomalies in the far western Pacific (around 130° E) occur in northern spring of year 0, leading those at the dateline by about one-half year. Third, not every westerly event occurring over the western Pacific all leads to an El Niño. Failed examples are found in 1980, 1990, and 1991 which were called "aborted" El Niños. A primary difference between the aborted El Niño and El Niño lies in the anomalous winds over the central Pacific between the dateline and 140° W. For all El Niños after 1956, except the 1976 event, the maximum anomalous westerlies occurred west of 170° E and exceed 1.5 $ms^{-1}$ with the giving filtering used in Fig. 8. On the contrary, for the aborted ones, the westerly anomalies were not extended into the central Pacific The relaxation of the easterly trades in the central Pacific marks the appearance of a Pacific basin-wide warming.

There are two questions need to be addressed. First, what causes the initial intensification and eastward propagation of the westerly anomalies over the warm pool? Second, what prohibits (or promotes) the westerly anomalies further extend eastward into the central Pacific? The discussion in this section will focus on the first question.

In the very strong 1982–1983 El Niño, the development and eastward propagation are particularly evident. The rainfall anomalies were phase locked with the westerly anomalies and traveled across nearly the entire Pacific basin. It was suggested that this eastward propagation results from an air-sea interaction process in which dynamic processes (advection and enhanced downwelling) play a dominant role (e.g., Gill and Rasmusson, 1983; Harrison and Schopf, 1984). The sustained anomalous eastward wind stresses not only increases eastward transport of warm water through intensifying the North and South Equatorial Countercurrent and slowing down the South Equatorial Current (Wyrtki, 1975), but also possibly inducing downwelling Kelvin waves which propagate into the eastern Pacific (Cane and Sarachik, 1976) and change the heat balance, leading to a warming. Theoretical studies have revealed various types of coupled instability that may explain ENSO development (Philander et al., 1984; Hirst, 1986; Neelin, 1991) and a delayed action oscillator mechanism that may be responsible for the reoccurrence of ENSO events (e.g., Battisti, 1988). In these theories the oceanic dynamical processes (advection by ocean upwelling and currents) play dominant roles in changing SST. These coupled-instability theories are particularly pertinent to the development of ENSO anomalies in the central and eastern Pacific. The intensification and eastward movement of the westerly anomalies, however, start west of the dateline where SSTs are almost uniformly higher than 28 °C (the warm pool) and the thermocline is deep. These oceanic conditions preclude the dominance of the above-mentioned dynamical processes in the coupled instability of the ocean-atmosphere system.

On the other hand, one should consider the contribution to the coupled instability of the thermodynamic processes that can effectively change SST in the warm pool. Let us assume that the pressure drop in the subtropics of each hemisphere and the intensification of the western Pacific anomalous cyclones in the onset and early

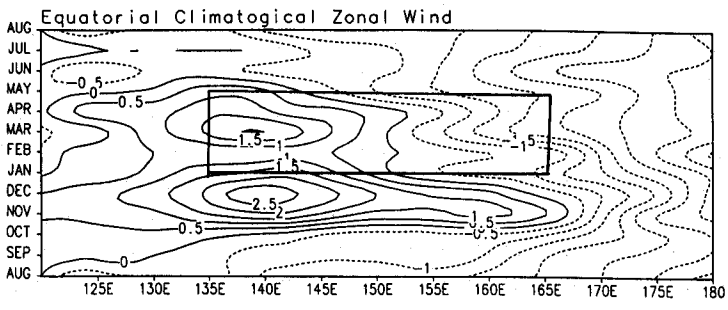


Fig. 8. Longitude-time diagram of the 9-month running mean anomalies of the zonal wind averaged between 5° N and 5° S, based on COADS. The contour inverval is 0.5 $ms^{-1}$. The box indicates the location and season that are most favorable for the proposed interactive instability to occur

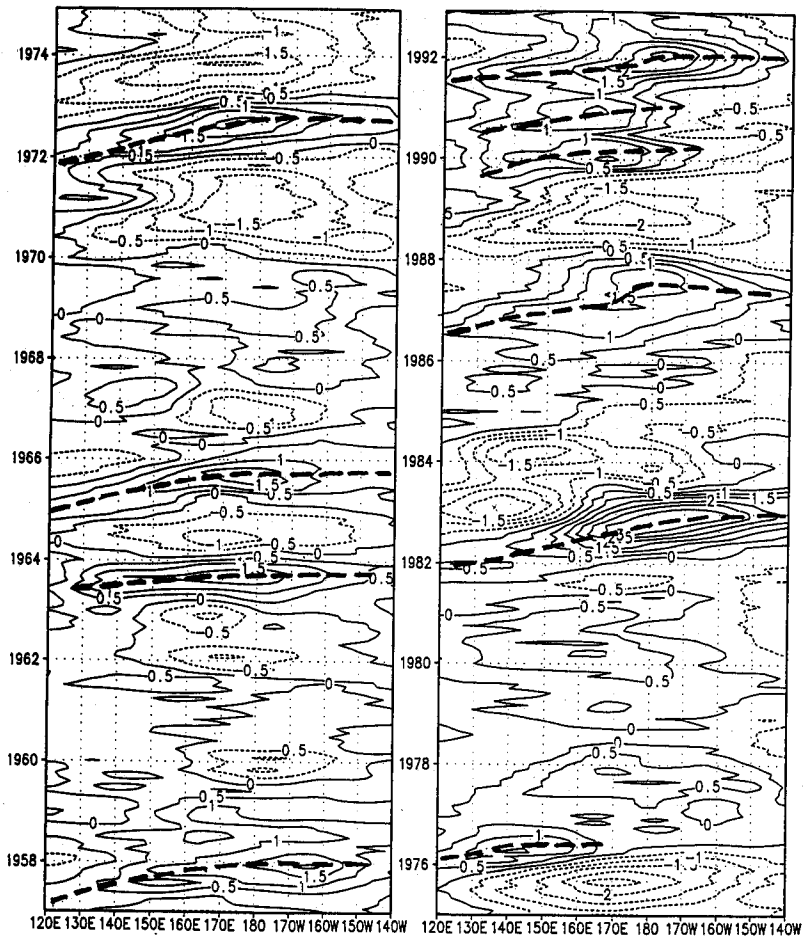


Fig. 9. Climatological monthly mean zonal wind speed ($ms^{-1}$) along the equator from 100° E to 140° W. The thick dashed lines indicate axes of the maximum westerly anomalies

development phases may introduce moderate westerly anomalies over the western equatorial Pacific. Assume that the monthly mean rates of evaporation cooling and turbulent mixing increase with increasing monthly mean surface wind speed. In the western equatorial Pacific the change of surface wind speed on interannual time scales is mainly due to the change of zonal wind component.

Both evaporational cooling and wind-induced turbulent mixing are among major processes that determine the interannual SST variation over the warm pool. Because the both processes depend on the total wind speed, especially the total zonal wind speed in the western equatorial Pacific, the response of SST to a moderate westerly anomaly would be affected by climatological mean winds in that region. In boreal spring, the climatological monthly mean zonal wind in the western equatorial Pacific varies from a weak westerly of 1–2 $ms^{-1}$ at 130–150° E to an easterly of about 3.5 $ms^{-1}$ near the dateline, with a reverse of direction around 150° E (Fig. 9). Superposition of a moderate equatorial westerly anomaly on the longitudinally varying mean winds can have quite different effects on SST at different longitudes. In the region of a weak mean easterly (160–170° E), a moderate westerly anomaly of 1–2 $ms^{-1}$ implies a reduction in the total wind speed. Thus, the cooling due to evaporation and turbulent mixing will be reduced, and an increase in SST is expected. In the region of a weak mean westerly (west of 150° E), on the other hand, a moderate westerly anomaly increases the total wind speed, which favors the cooling of the ocean surface through enhanced evaporation, turbulent mixing, erosion of the salinity "barrier layer", and entrainment at the mixed layer base (Meyers et al., 1986).

The cooling in the far western Pacific and the warming east of 155° E would create a moderate eastward SST gradient along the equator. In the warm pool where a large area is covered by SST greater than 28 °C, deep convection is enhanced in areas where SST exceeds 28 °C (Fu et al., 1990). Thus anomalous convection would be enhanced

east of 155° E. Due to the small moist static stability of the atmosphere over the warm pool, the anomalous convection would induce a negative pressure anomaly (Wang, 1992). In addition, the SST gradient can directly generate a hydrostatic pressure gradient via differential surface buoyancy flux (Lindzen and Nigam, 1987). Because of the great sensitivity of the zonal wind to an equatorial pressure gradient, a moderate eastward SST gradient could effectively reinforce westerlies to the east of the maximum cooling (or the maximum westerly anomalies), causing eastward propagation of the westerly anomalies. This process involves a slow positive feedback between zonally differential oceanic heating and the boundary layer winds. It may be potentially important in the warm pool where SST fluctuation is not directly controlled by an equatorial upwelling or horizontal advection. The nature of the coupling is, therefore, fundamentally different from that which occurs in the eastern equatorial Pacific.

## 6. Discussions

During the transition periods, both the atmosphere and ocean are in normal climatological (annual cycle) conditions. The local coupling between the tropical atmosphere and ocean is weak, because the annual cycle, to a large extent, is determined by insolational forcing, especially in the western Pacific. Even in the tropical eastern Pacific where air-sea interaction is involved, the insolational forcing still fundamentally regulates the annual cycle (Wang, 1994a). As a direct consequence of this weak coupling, relatively high frequency (intraseasonal to annual time-scales) disturbances, perhaps primarily in the extratropical atmosphere, could interfere with the ENSO mode and cause irregularities in the ENSO cycle.

The occurrence of minimum pressure anomalies in the subtropics around the node line of the Southern Oscillation leads the central Pacific warming (mature phase of an ENSO event) by about one year. This is probably the most conspicuous precursor for the onset of a warm episode. Both the location and the season are critical for the pressure fall to be in effect. This pressure fall favors the formation of anomalous cyclones and the establishment of equatorial westerly anomalies over the western Pacific. It is not a passive atmospheric response to tropical Pacific SST anomalies, because the latter are small in the onset phase. This pressure drop is likely linked to abnormal annual cycle in the atmosphere outside the tropics and serves as a mechanism that causes irregularities in the ENSO evolution. It is unclear, however, exactly what is responsible for the subtropical pressure fall in boreal fall and winter of year $-1$, which may play an important role in the initiation of the coupled ocean/atmosphere instability in the western-central Pacific.

A common feature of the development of basin-wide warming for all significant El Niños in the last four decades was the establishment of equatorial westerly anomalies in the western Pacific and subsequent slow eastward propagation from boreal spring to winter of the El Niño year. It is hypothesized that this common development process results from the effects of zonal variations of the mean winds along the equator and the oceanic thermodynamic processes, by which westerly anomalies create an east-west SST gradient and the SST gradient in turn feeds back to the surface winds.

For the proposed mechanism to work, the zonal structure of the mean winds at the equator is a critical factor. In this regard, both the geographic location and the season are important elements. Geographically, the most favorable location is the equatorial Pacific between 135° E and 165° E. This area is the core of the warm pool and has virtually no east-west SST gradient nearly all year round (see Sadler et al., 1987 for instance). Seasonally, the most favorable seasons are boreal winter and spring, in particular from January to April. During this period the climatological equatorial winds are light (monthly mean wind speed is less than 2 $ms^{-1}$), yet have relatively large zonal variation (about 3 $ms^{-1}$ per 20° longitude) (Fig. 8). In fact, the onset and development of El Niños are characterized by the occurrence of equatorial westerly anomalies in this area during the boreal winter and spring. The most evident slow eastward propagation of the equatorial westerly anomalies also takes place in this area (Fig. 5). These observations appear to support the hypothesis. The occurrence of equatorial westerly anomalies over the core of the warm pool, however, is probably only a necessary (or favorable) condition, but not sufficient. For instance, significant anomalous westerlies occurred over the western equatorial Pacific in early 1980 and early 1990 (Figs. 7c and 8), the western-central Pacific during these two

years experienced abnormal warming, but the warming did not spread into the eastern Pacific. Apparently, there are other factors that may also affect the proposed interactive instability in the western Pacific. Further studies are required to find out these factors.

In addition to the common features, differences between the cases in the transition are notable. The characteristic evolution of SST anomalies has changed notably since the late 1970s (Fig. 2). The causes of the changes are discussed in an accompanying paper (Wang, 1994b). Another secular change was noticed in the evolution of SLP anomalies. While the lowest pressure anomalies associated with El Niño in the southeast Pacific tend to be quasi-stationary, the highest pressure anomalies over the Maritime Continent exhibit a significant northeastward propagation before, during, and after the central Pacific peak warming (Fig. 4). The propagation path of the highest SLP anomalies changed in the late 1960s. The causes of these changes call for further investigations.

**Acknowledgments**

The author wishes to thank Dr. Julian Wang at CAC/NMC for sharing his data, and Y. He, Y. Wang, and D. Kessler for their technical assistance. This research has been supported by the NOAA EPOCS program.

**References**

Barnett, T. P., 1981: Statistical relations between ocean/atmosphere fluctuations in the tropical Pacific. *J. Phys. Oceanogr.*, **11**, 1043–1058.

Barnett, T. P., 1983: Interaction of the monsoon and Pacific trade wind systems at interannual time scales. Part I: The equatorial zone. *Mon. Wea. Rev.*, **111**, 756–773.

Barnett, T. P., 1984: Interaction of the monsoon and Pacific trade wind system at interannual time scales. Part III: A partial anatomy of the Southern Oscillation. *Mon. Wea. Rev.*, **112**, 2388–2400.

Barnett, T. P., 1985: Variations in near global sea level pressure. *J. Atmos. Sci.*, **42**, 478–501.

Battisti, D. S., 1988: The dynamics and thermodynamics of a warm event in a coupled tropical atmosphere/ocean model. *J. Atmos. Sci.*, **45**, 2889–2919.

Bjerknes, J., 1966: A possible response of the atmospheric Hadley circulation to equatorial anomalies of ocean temperature. *Tellus*, **18**, 820–829.

Bjerknes, J., 1969: Atmospheric teleconnections from the equatorial Pacific. *Mon. Wea. Rev.*, **97**, 163–172.

Busalacchi, A., O'Brien, J. J., 1981: Interannual variability of the equatorial Pacific in the 1960's. *J. Geophys. Res.*, **86**, 10901–10907.

Cane, A. M., 1993: Tropical Pacific ENSO models: ENSO as a mode of the coupled system. In: Trenberth, K. E. (ed.) *Climate System Modelings*. New York: Cambridge University Press, pp. 788.

Cane, A. M., Sarachik, E. S., 1977: Forced baroclinic ocean motion: II. *J. Mar. Res.*, **35(2)**, 395–432.

Fu, R., Del Genio, A. D., Rossow, W. B., 1990: Behavior of deep convective clouds in the tropical Pacific deduced from ISCCP radiances. *J. Climate*, **3**, 1129–1152.

Gill, A. E., Rasmusson, E. M., 1983: The 1982–1983 climate anomaly in the equatorial Pacific. *Nature*, **306**, 229–234.

Gutzler, D. S., Harrison, D. E., 1987: The structure and evolution of seasonal wind anomalies over the near-equatorial eastern Indian and western Pacific Oceans. *Mon. Wea. Rev.*, **115**, 169–192.

Hackert, E. C., Hastenrath, S., 1986: Mechanisms of Java rainfall anomalies. *Mon. Wea. Rev.*, **114**, 745–757.

Harrison, D. E., Schopf, P. S., 1984: Kelvin-wave-induced anomalous advection and the onset of surface warming in El Niño events. *Mon. Wea. Rev.*, **112**, 923–933.

Hirst, A. C., 1986: Unstable and damped equatorial modes in simple coupled ocean-atmospheric model. *J. Atmos. Sci.*, **43**, 606–630.

Keen, R. A., 1982: The role of cross-equatorial cyclone pairs in the Southern Oscillation. *Mon. Wea. Rev.*, **110**, 1405–1416.

Kiladis, G. N., van Loon, H. 1988: The Southern Oscillation. Part VII: Meterological anomalies over the Indian and Pacific sectors associated with the extremes of the oscillation. *Mon. Wea. Rev.*, **116**, 120–136.

Lau, K. M., Chang, C.-P., Chan, P. H., 1983: Short-term planetary-scale interactions over the tropics and midlatitudes. Part II: Winter MONEX period. *Mon. Wea. Rev.*, **111**, 1372–1388.

Lau, K. M., Chan, P. H., 1986: Aspects of the 40–50 day oscillation during the northern summer as inferred from outgoing longwave radiation. *Mon. Wea. Rev.*, **114**, 1354–1367.

Lindzen, R. S., Nigam, S., 1987: On the role of sea surface temperature gradients in forcing low-level winds and convergence in the tropics. *J. Atmos. Sci.*, **45**, 2440–2458.

Meehl, G. A., 1987: The annual cycle and interannual variability in the tropical Pacific and Indian Ocean region. *Mon. Wea. Rev.*, **115**, 27–50.

Meyers, G., Donguy, J. R., Reed, R. K., 1986: Evaporative cooling of the western equatorial Pacific Ocean by anomalous winds. *Nature*, **323**, 523–526.

Neelin, J. D., 1991: The slow sea surface temperature mode and the fast wave limit: analytical theory for tropical interannual oscillations and experiments in a hybrid coupled model. *J. Atmos. Sci.*, **48**, 584–606.

Philander, S. G., 1981: The response of equatorial oceans to a relaxation of the trade winds. *J. Phys. Oceanogr.*, **11**, 176–189.

Philander, S. G., 1985: El Niño and La Nina. *J. Atmos. Sci.*, **42**, 2652–2662.

Philander, S. G. H., Yamagata, T., Pacanoski, R. C., 1984: Unstable air-sea interactions in the tropics. *J. Atmos. Sci.*, **41**, 604–613.

Philander, S. G., Rasmusson, E. M., 1985: The Southern Oscillation and El Niño. *Adv. Geophys.*, **28A**, 197–215.

Rasmusson, E. M., Carpenter, T. H., 1982: Variations in tropical sea surface temperature and surface wind fields associated with the Southern Oscillation/ El Niño. *Mon. Wea. Rev.*, **110**, 354–384.

Sadler, J. C., Lander, M. A., Hori, A. M., Oda, L. K., 1987: Tropical marine climate atlas. Vol. 2: Pacific Ocean. Report UHMET 87-02, Department of Meteorology, University of Hawaii, Honolulu, Hawaii, 27pp.

Sharpiro, R., 1970: Smoothing, filtering, and boundary effects. *Rev. Geophys. Space Phys.*, **8**, 359–387.

Trenberth, K. E., Shea, D. J., 1987: On the evolution of the Southern Oscillation. *Mon. Wea. Rev.*, **115**, 3078–3096.

van Loon, H., Shea, D. J., 1985: The Southern Oscillation. Part IV: The precursors south of 15° S to the extremes of the oscillation *Mon. Wea. Rev.*, **113**, 2063–2074.

van Loon, H., Shea, D. J., 1987: The Southern Oscillation. Part VI: Anomalies of sea level pressure on the southern hemisphere and of Pacific sea surface temperature during the development of warm event. *Mon. Wea. Rev.*, **115**, 370–379.

Wang, B., 1992: The vertical structure and development of the ENSO anomaly mode during 1979–1989. *J. Atmos. Sci.*, **49**, 698–712.

Wang, B., 1994a: On the annual cycle in the tropical eastern-central Pacific. *J. Climate*, **7**, 1926–1942.

Wang, B., 1994b: Changes in the El Niño onset in the last four decades. *J. Climate* (in press).

Wyrtki, K., 1975: El Niño-the dynamic response of the equatorial Pacific Ocean to atmospheric forcing. *J. Phys. Oceanogr.*, **5**, 572–584.

Wyrtki, K., 1982: The Southern Oscillation, ocean-atmosphere interaction and El Niño. *Marine Technol. Soc. J.*, **16**, 3–10.

Yasunari, T., 1985: Zonally propagating modes of the global west circulation associated with the Southern Oscillation. *J. Meteor. Soc. Japan.*, **63**, 1013–1029.

Yasunari, T., 1990: Impact of the Indian monsoon on the coupled atmosphere/ocean system in the tropical Pacific. *Meteorol. Atmos. Phys.*, **44**, 29–41.

Author's address: B. Wang, Department of Meteorology, School of Ocean and Earth Science and Technology, University of Hawaii, 2525 Correa Road, Honolulu, Hawaii 96822, U. S. A.